

Relation Between Shear Rate and Structural Parameter in Non-Newtonian Droplet Oscillations via Jacobi Sets and STL Decomposition: A Visual Analysis

D. Klötzl^{*1}, M. Ibach², B. Weigand², D. Weiskopf¹

¹Visualization Research Center (VISUS), University of Stuttgart, Stuttgart, Germany

²Institute of Aerospace Thermodynamics (ITLR), University of Stuttgart, Stuttgart, Germany

^{*}Corresponding author: daniel.kloetzl@visus.uni-stuttgart.de

Keywords

DNS, VOF, Multiphase, Droplet Oscillation, Non-Newtonian, Thixotropy, Jacobi Sets, STL

Introduction

Liquids with a non-Newtonian rheological behavior are frequently encountered in engineering applications, such as coating, polymer processing, and oil drilling. Thixotropy is a scarcely investigated non-Newtonian behavior in which the fluid's viscosity depends on the shear rate and the deformation history. Understanding the rheological behavior of thixotropic fluids is essential in applications, but it is challenging to quantify and examine involved processes and mechanisms separately in experiments. Therefore, numerical simulation can be used to characterize and quantify the fluid behavior.

The main objective of this work is to reveal the relationships between the fluid structure and the flow field inside a thixotropic fluid droplet by analyzing data of the fundamental case of an oscillating droplet consisting of an ideal thixotropic fluid. To this end, we use the in-house multiphase flow solver Free Surface 3D (FS3D) [1,2]. The analysis is conducted with the two methods: Jacobi sets, introduced by Edelsbrunner et al. [3], a mathematical tool that captures gradient alignments of multiple scalar fields, and seasonal-trend decomposition based on loess (STL) by Cleveland et al. [4], a method used to analyze and extract trends and seasonal patterns in time series data.

The first goal of this study is to investigate the interdependence of shear rate and structural parameter, which characterizes the integrity of the thixotropic fluid, using the improved Jacobi set computation method by Klötzl et al. [5, 6] to better understand the governing processes. The second goal is to use STL decomposition to analyze and extract trends and seasonal patterns for different parameters that control the recovery and breakdown of the fluid structure. The tools in this study can be used to present data from the parametric study and expose fundamental connections between the fluid structure and flow field. Moreover, the methods introduced here can be applied to derive appropriate correlations essential for designing and optimizing various industrial processes involving thixotropic fluids.

Dataset and Methods

The numerical modeling of the evolution of the structural parameter λ is computed via the transport kinetic equation

$$\underbrace{\frac{\partial \lambda}{\partial t} + \mathbf{u} \cdot \nabla \lambda}_{\text{Advection}} = \underbrace{-k_1 \dot{\gamma} \lambda}_{\text{Breakup}} + \underbrace{k_2(1 - \lambda)}_{\text{Rebuilding}}, \quad (1)$$

introduced by Moore [7], in combination with the constitutive equation for the viscosity

$$\eta_a(\lambda) = \eta_\infty(1 + \alpha\lambda), \quad (2)$$

using FS3D, see [2]. Here, the structural parameter λ varies between 0 and 1, where $\lambda = 0$ corresponds to a completely broken and $\lambda = 1$ to a fully recovered microstructure. The shear rate is denoted via $\dot{\gamma}$, the breakdown strength and recovery rate are given via k_1 and k_2 , respectively. For the apparent viscosity $\eta_a(\lambda)$ that is linked to the infinite shear viscosity η_∞ and the zero-shear viscosity $\eta_\infty(1 + \lambda)$, the special cases of $\alpha = 0$ (no effect on the viscosity of the droplet) and $\alpha = 99$ (a link between the structural parameter and the droplet's viscosity) are investigated. We compare different configurations of the non-dimensional parameters k_1 and the mutation number $\text{Mu} = k_2 \cdot T_{sim}$ with the oscillation period of the droplet used as a characteristic time scale.

For the visual analysis, we use the Jacobi set and STL separately. In the special case of two-dimensional scalar-valued functions $f, g \in \mathbb{R}^2 \supset M \rightarrow \mathbb{R}$, the Jacobi set can be defined via $J(f, g) := \{x \in M: \nabla f \times \nabla g = 0\}$, thus it captures gradient alignments of given scalar fields. In the second analysis, the time series was decomposed additively into a trend, seasonal (according to the period T_{sim}), and residual component. This decomposition is illustrated for the example of the evolution of the structural parameter λ over the non-dimensional time for $k_1 = 10$ (blue) and $k_1 = 40$ (red) in Figure 1.

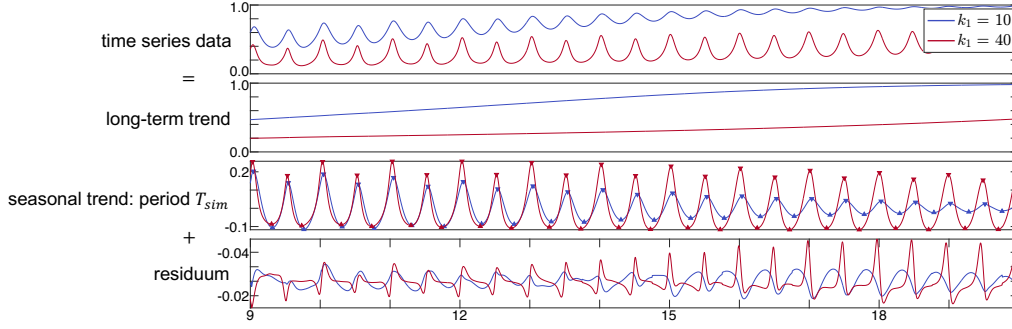


Figure 1. STL decomposition of the evolution of the structural parameter λ over the non-dimensional time $\tilde{t} = t/T_{sim}$ for $k_1 = 10$ (blue) and $k_1 = 40$ (red), $Mu = 10$ with highlighted min/max in the seasonal component.

Results and Discussion

In Figure 2, the droplets are given at time $\tilde{t} = 0.43$ (top) and $\tilde{t} = 2.43$ (bottom). The shear rate $\dot{\gamma}$ and the structural parameter $\lambda \in [0,1]$ for $Mu = 10$ are used as the two input scalar fields for the Jacobi set for the cases of $k_1 = 10$ (left) and $k_1 = 0.1$ (right). The corresponding scalar fields are visualized via two colormaps in the background and the current flow field inside the droplet via line integral convolution (LIC) [8]. The Jacobi sets (black/white lines) for these specific time steps differ for different k_1 values. The comparison of the numerical results reveals that the Jacobi sets show similar results in two-thirds of the regarded time steps. From this exploration, an analytic investigation of the Jacobi set dependence between the structural parameter and the shear rate could lead to an analytic dependence. Another possible research direction could be the analysis of the interdependence between Jacobi set and varying k_1 and Mu values of the breakup and rebuilding of the fluid structure.

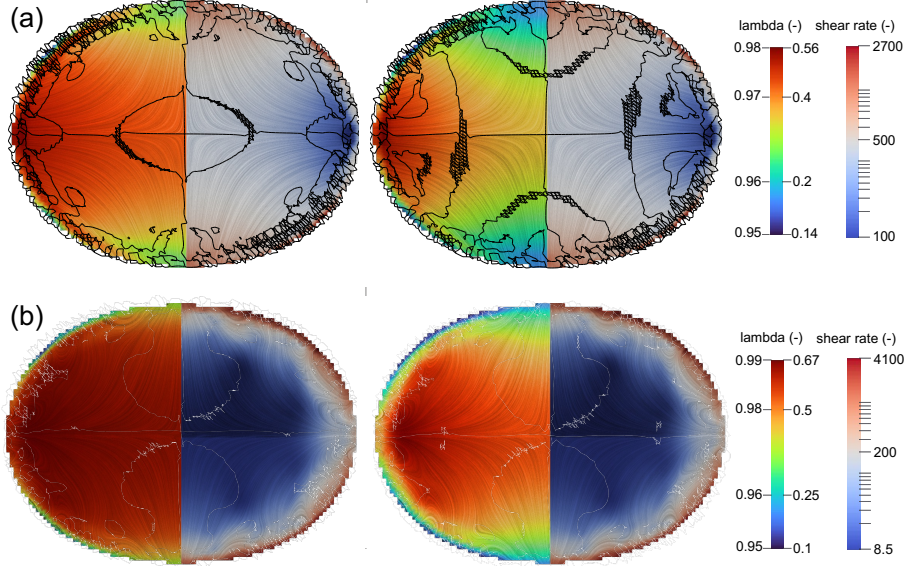


Figure 2. Jacobi set (black/white lines) of the shear rate $\dot{\gamma}$ and the structural parameter $\lambda \in [0,1]$ for $Mu = 10$: (a) at time $\tilde{t} = 0.43$ for $\alpha = 0$ (left: $k_1 = 10$, right: $k_1 = 0.1$) and (b) at time $\tilde{t} = 2.43$ for $\alpha = 0$ (left: $k_1 = 10$, right: $k_1 = 0.1$).

For the second part, we discuss the results of the decomposition of the averaged structural parameter λ using STL. Here, the evolution of the structural parameter λ over the non-dimensional time \tilde{t} is decomposed into a trend, seasonal, and absolute residual component. This decomposition is given in Figure 3 for different mutation numbers 0.1 and 10 (on the left) as well as 1 and 100 (on the right) for a range of k_1 values between 0.01 and 100. The k_1 values are visually encoded using different colors from a discrete warm cold color scale. Furthermore, two detailed zoomed-in areas of the seasonal and residual components of the mutation numbers 1 and 10 are given.

In the analysis, the STL decomposition simplifies the comparison of the oscillation heights between the different configurations since one can directly compare the seasonal patterns to each other. This confirms the results from Ibach et al. [2] that the maxima of the averaged structural parameter λ lie ahead of the maxima of the oscillating modes. Moreover, one can state that the higher the breakdown strength k_1 , the more distinct the shift between the maxima is. This is especially emphasized in the zoomed-in areas for the mutation numbers 1 and 10.

The numerical exact evaluation of the decomposed structural parameter's maxima shift in comparison to the oscillation modes could be of interest for further investigation in the future.

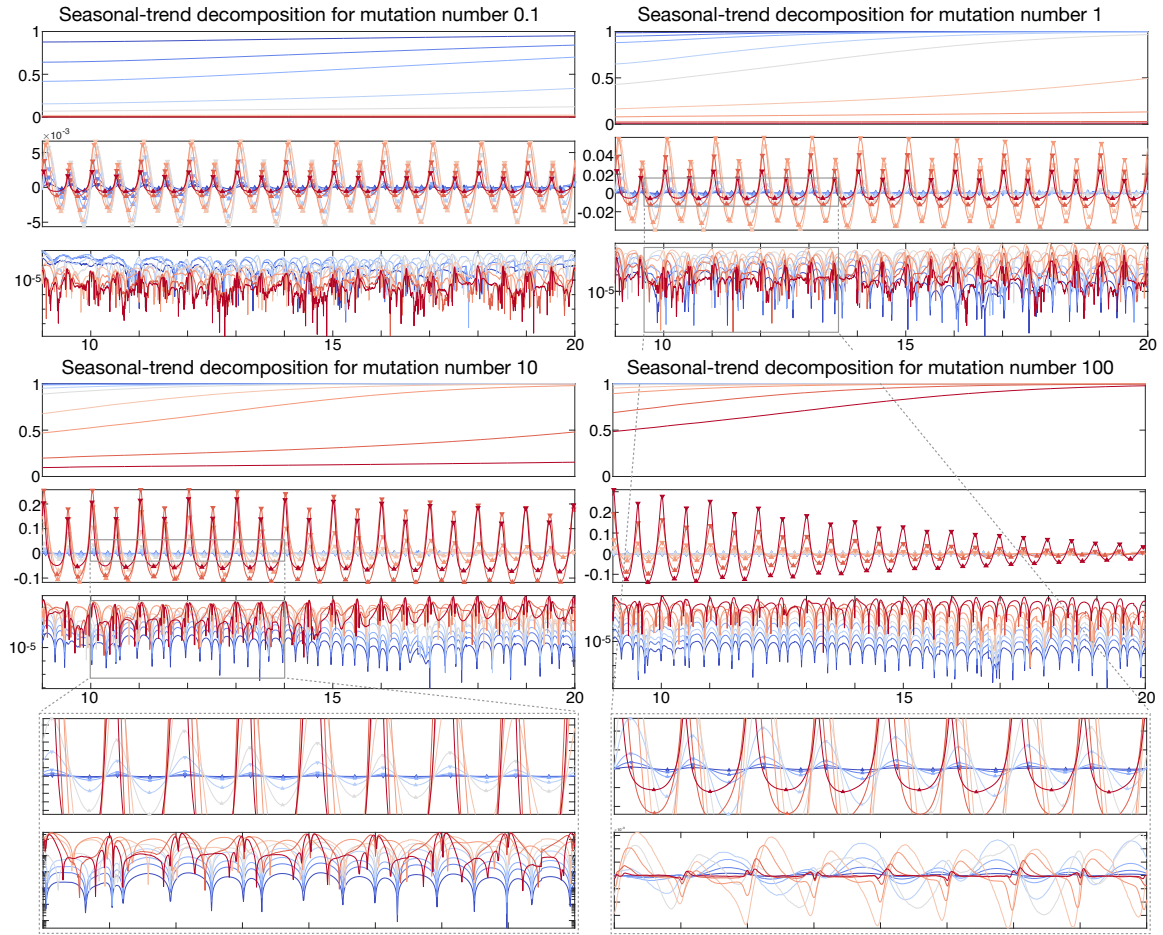


Figure 3. STL decomposition of the evolution of the structural parameter λ over the non-dimensional time \tilde{t} for the mutation numbers 0.1 and 10 (left) as well as 1 and 100 (right). The different k_1 values are visually encoded in the discrete warm cold color scale. Zoomed-in areas highlight two specific regions of the resulting seasonal and residual components (upper and lower part, respectively).

Acknowledgments

This work was supported by the Deutsche Forschungsgemeinschaft (DFG, German Research Foundation) – Project-ID 270852890 – GRK 2160/2 and under Germany’s Excellence Strategy – EXC 2075 – 390740016. We also acknowledge the support by the Stuttgart Center for Simulation Science (SimTech) and the High-Performance Computing Center Stuttgart (HLRS) for the support and the supply of computational resources on the HPE Apollo (Hawk) platform under Grant No. FS3D/11142.

References

- [1] K. Eisenschmidt, M. Ertl, H. Goma, C. Kieffer-Roth, C. Meister, P. Rauschenberger, M. Reitzle, K. Schlottke, and B. Weigand, “Direct numerical simulations for multiphase flows: An overview of the multiphase code FS3D,” *Appl Math Comput*, vol. 272, pp. 508–517, 2016.
- [2] M. Ibach, J. Steigerwald, and B. Weigand, “Thixotropic effects in oscillating droplets,” in *11th International Conference on Multiphase Flows*, Kobe, Japan, 2023.
- [3] H. Edelsbrunner and J. Harer, “Jacobi sets of multiple Morse functions,” in *Found Comput Math*, pp. 37–57, 2002.
- [4] R. B. Cleveland, W. S. Cleveland, J. E. McRae, and I. Terpenning, “STL: A seasonal-trend decomposition,” *J Offic Stat*, vol. 6, no. 1, pp. 3–73, 1990.
- [5] D. Klötzl, T. Krake, Y. Zhou, I. Hotz, B. Wang, and D. Weiskopf, “Local bilinear computation of Jacobi sets,” *Vis Comput*, vol. 38, no. 9, pp. 3435–3448, 2022.
- [6] D. Klötzl, T. Krake, Y. Zhou, J. Stober, K. Schulte, I. Hotz, B. Wang, and D. Weiskopf, “Reduced connectivity for local bilinear Jacobi sets,” in *2022 Topological Data Analysis and Visualization (TopoInVis)*, pp. 39–48, 2022.
- [7] F. Moore, “The rheology of ceramic slips and bodies,” *Trans Br Ceram Soc* 58, pp. 470–494, 1959.
- [8] B. Cabral and L. C. Leedom, “Imaging vector fields using line integral convolution,” in *Proceedings of the 20th Annual Conference on Computer Graphics and Interactive Techniques*, pp. 263–270, 1993.